PHYSICAL REVIEW
LETTERS

VOLUME 12 22 JUNE 1964 NUMBER 25

EXCITATION OF LONGITUDINAL PLASMA OSCILLATIONS NEAR ELECTRON CYCLOTRON HARMONICS

S. J. Buchsbaum and A. Hasegawa
Bell Telephone Laboratories, Murray Hill, New Jersey
(Received 22 May 1964)

We have studied microwave absorption in a plasma column near the harmonics of the electron cyclotron frequency and have found that it exhibits structure (the peaks $a, b, c, d, \cdots$ in Fig. 1) which consists of many lines as a function of static magnetic field. Similar, but less prominent, lines were also reported in microwave emission.[1] The origin of this resonant structure has not been understood heretofore. In this note we present the observed properties of these resonances and develop the theory for them. We attribute the resonances to excitation of longitudinal plasma oscillations within narrow pass-bands near each cyclotron harmonic. Such pass-bands were discussed by Bernstein[2] for propagation of electrostatic oscillations across a static magnetic field. We will show, however, that as in the case of oscillations in the absence of a magnetic field (the so-called Tonks-Dattner resonances[3,4]) the dispersion relation and the nature of the oscillations are profoundly modified by density gradients. We believe that such oscillations play an important role in the many reported instances of very large emission of microwave radiation near cyclotron harmonics.

The nature of oscillations in the presence of a magnetic field differs in the following essential way from Tonks-Dattner resonances. The latter ones can be excited only at frequencies larger than the local plasma frequency.[3,4] Consequently, in a plasma column of finite radius, whose density decreases from the axis towards the walls, the Tonks-Dattner oscillations are confined to a narrow annular region near the wall of the tube, where the plasma frequency is below the oscillation frequency. As shown most impressively by Nickel, Parker, and Gould[3] and by others,[4] the

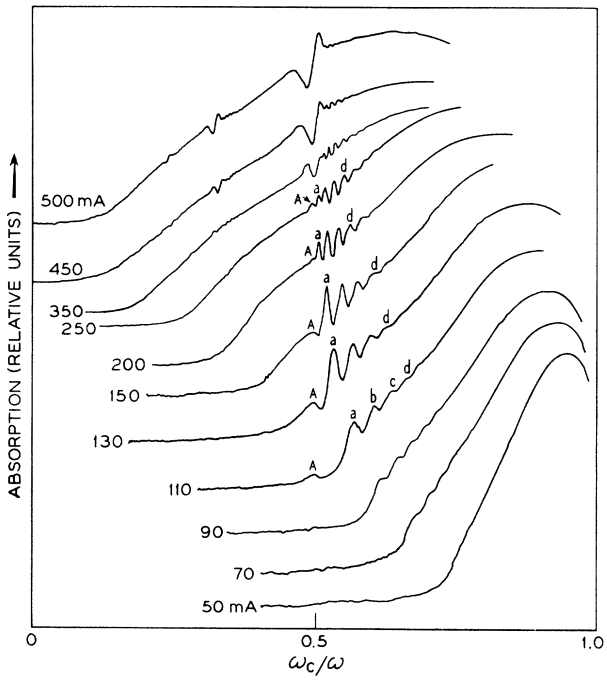

FIG. 1. Microwave absorption (in relative units) in a plasma column as a function of magnetic field with current I as a parameter. Pressure = 0.3 Torr. The curves for different I's are displaced for display purposes.

actual frequency spectrum depends strongly on the nature of density gradients in and near the sheath. In the presence of a magnetic field, plasma oscillations can be excited at frequencies lower than subharmonics of the electron cyclotron frequency,[2] provided the plasma frequency exceeds a certain critical value (which is a function of magnetic field). These oscillations are thus confined to a region near the axis of the plasma column and are relatively insensitive to conditions in the sheath. They are responsible for the resonances shown in Fig. 1.

The absorption spectrum reproduced in Fig. 1 was obtained as follows. The positive column (8 mm in diameter) of a hot-cathode arc discharge in helium was inserted coaxially into a cylindrical cavity oscillating in a TE_{011} mode. The resonant frequency of the empty cavity was 5000 Mc/sec. A static magnetic field uniform over the volume of the plasma to better than 0.5% was applied parallel to the axis of plasma column, and the microwave absorption by the plasma was measured as a function of the magnetic field (keeping the microwave frequency on cavity resonance) by monitoring the microwave power transmitted through the cavity. The TE_{011} mode simulates very well the interaction of a cylindrical extraordinary wave propagating radially in a plasma column.[5] The broad absorption background results from the cold-plasma resonance at $\omega^2 = \omega_p^2 + \omega_c^2$; its shape is governed by radial density gradients within the plasma column.[6] Superimposed on this background absorption is the resonant structure under discussion here. The peak A is not part of the series of peaks a, b, c, etc. It is thought to result from resonant absorption of the extraordinary electromagnetic wave itself, perhaps because of anharmonic motion of electrons in the sheath.[7] At constant microwave and plasma frequencies, the series of peaks $a, b, c, d, \cdots$ appears at fields higher than $B = m\omega/en$ where $n = 2, 3, 4, \cdots$. Their amplitude is largest for $n = 2$, but they are still clearly discernible for $n = 3$ and 4. As the plasma frequency is increased, the lines crowd closer. This experimentally observed behavior is plotted in Fig. 2(a). We determined experimentally that the position of the peaks $a, b, c, d, \cdots$ was insensitive to variation of the length of the plasma column that was exposed to microwaves. This suggests that the peaks resulted from excitation of radial rather then axial modes within the plasma column.

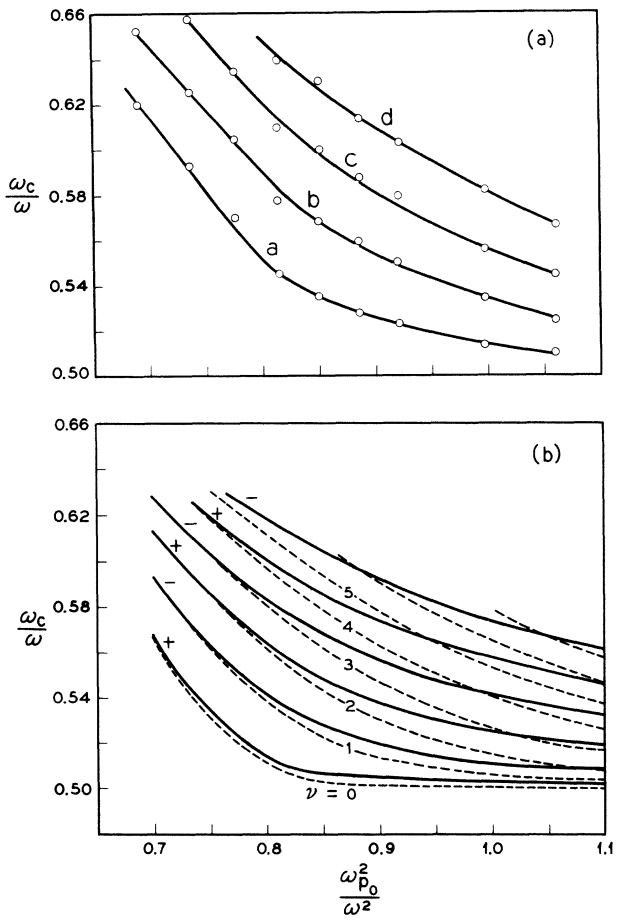

FIG. 2. (a) Position of peaks of a, b, c, $\cdots$ of Fig. 1 as a function of ω_{p0}^2/ω^2. The values of ω_{p0}^2 are deduced from the onsets of cold-plasma absorption in Fig. 1 due to resonance at $\omega^2 = \omega_c^2 + \omega_p^2$. (b) Calculated resonant frequencies of the odd (-) and even (+) solutions in a plasma slab. The solid lines are the solution of Eq. (6) and the dotted lines are given by $\nu + 1 = n$, $n = 1, 2, \cdots$.

In order to account quantitatively for this resonant structure we adopt the following model. The cylindrical plasma column is replaced by a plasma slab with its faces at $x = \pm l$. The density is assumed to vary such that $\omega_p^2 = \omega_{p0}^2 g(x)$ where ω_{p0}^2 is the plasma frequency at $x = 0$ and $g(0) = 1$. The dc magnetic field is along the z axis and the oscillations propagate only along x, that is, in the direction along which there is a density gradient. This model proved sufficient to account for most aspects of the Tonks-Dattner resonances in the absence of a magnetic field.[4] It has the great virtue that for certain quite realistic $g(x)$, closed-form solutions will prove possible.

Unlike the case with no magnetic field it is not

sufficient to use the first two moments of the Boltzmann equation to describe the particle density and current. To bring out the resonant features near cyclotron harmonics, the linearized Boltzmann equation must be employed.[8] This equation may be formally integrated if the spatial derivative d/dx is retained as an operator.[9]

If the width of the plasma slab, $2l$, is much larger than the Larmor radius, the perturbed distribution function may be expanded with $(u/\omega_C) \times (d/dx)$ as the expansion parameter, where $u^2 = eT/m$ with T the temperature. To study the absorption near $\omega \approx 2\omega_C$ it is sufficient to take those terms in the expansion which are linear in the temperature T.[10] The use of the distribution function in Poisson's equation yields

$$\frac{d^2y}{dx^2} + \frac{1}{\lambda^2}\left(\mathcal{E} - \frac{1}{g(x)}\right) y = 0 \qquad (1)$$

where $y = g(x)d\varphi/dx$, φ is electrostatic potential, and

$$\frac{1}{\lambda^2} = \frac{(\omega^2 - \omega_c^2)(4\omega_c^2 - \omega^2)}{(3eT/m)\omega_{p0}^2},$$

and

$$\mathcal{E} = \frac{\omega_{p0}^2}{\omega^2 - \omega_c^2}.$$

Note that λ^2 and $\mathcal{E}$ are positive when $\omega_C < \omega < 2\omega_C$. Equation (1) has the form of a Schrödinger wave equation with $\mathcal{E}$ and $g(x)^{-1}$ being regarded as kinetic and potential energy, respectively. For a uniform density, $g(x) = 1$, the solutions are sinusoids, with eigenvalues such that $(\mathcal{E} - 1) = \lambda^2(n\pi/2l)^2$, or

$$(4\omega_c^2 - \omega^2)(\omega_c^2 - \omega_p^2 - \omega^2) - \left(\frac{3eT}{m}\right)\omega_p^2\left(\frac{n\pi}{2l}\right)^2 = 0, \qquad (2)$$

with $n = 1, 2, \cdots$. Equation (2) is nearly, but not quite, sufficient to account for the experimental results. It fails mainly in that it predicts too small a spacing between the resonant lines increasing as n^2 while the experimentally observed lines are nearly uniformly spaced.

As in the Tonks-Dattner case, this discrepancy is resolved by taking account of density variation along x. We take $1/g(x) = 1 + \gamma(x/l)^2$ as a good approximation for the actual density variation in the plasma. Then Eq. (1) is immediately soluble in terms of the parabolic cylinder function[11] as

$$y_\pm = c_1[D_\nu(x/c) \pm D_\nu(-x/c)], \qquad (3)$$

where

$$c = \left[\frac{3\omega_{p0}^2(eT/m)l^2}{4\gamma(\omega^2 - \omega_c^2)(4\omega_c^2 - \omega^2)}\right]^{1/4} \qquad (4)$$

and

$$\nu = \frac{1}{2}\left[\left\{\frac{(4\omega_c^2 - \omega^2)l^2}{3\gamma\omega_{p0}^2(eT/m)(\omega^2 - \omega_c^2)}\right\}^{1/2} \times (\omega_c^2 + \omega_{p0}^2 - \omega^2) - 1\right]. \qquad (5)$$

The function $D_\nu(x/c)$ has $\nu + 1$ zeros. It vanishes exponentially for large x/c, that is, it exhibits a wave-like behavior near $x \simeq 0$ [actually where $\mathcal{E} - 1 - \gamma(x/l)^2 > 0$], and a "tunneling"-like behavior of a particle trapped in a parabolic potential well for large x/c, that is, for x near l.

The eigenvalues λ are obtained by applying the boundary condition that $y_\pm$ vanishes at $x = \pm l$,

$$D_\nu(l/c) \pm D_\nu(-l/c) = 0. \qquad (6)$$

Equation (6) is solved for ω_C/ω as a function of ω_{p0}^2/ω^2 and shown in Fig. 2(b) (as solid curves) for $T = 10$ eV, $l = 2.5$ mm, and $\gamma = 0.25$. As $[D_\nu(x) + D_\nu(-x)]$ and $[D_\nu(x) - D_\nu(-x)]$ are even and odd functions, respectively, the "+" curves represent the even and the "-" curves the odd solutions.

For certain values of ω_{p0} approximate solutions with a simple physical interpretation may be constructed. For small ω_{p0}, $\mathcal{E}$ is small and $[\mathcal{E} - \gamma(x/l)^2 - 1]$ is negative. As ω_{p0} is increased, $[\mathcal{E} - \gamma(x/l)^2 - 1]$ becomes positive but only near $x = 0$. Then, the wave is trapped by the potential well and is quantized by it rather than by the walls at $x = \pm l$. Such quantization condition is $\nu + 1 = n$, where $n = 1, 2, \cdots$. The dotted curves in Fig. 2(b) show the results of such quantization with ν obtained from Eq. (5). It can be seen that the approximate solution very well approximates the exact one at low ω_{p0}. As ω_{p0} increases, the boundary at $x = \pm l$ becomes more and more important and dotted curves deviate from the solid ones. However, the spacings of the curves in ω_C/ω remain fairly uniform because the zeros of $D_\nu(x)$ crowd closer for large x. In the approximate solutions there is only one independent parameter, $l^2/\gamma T$.

The agreement between the observed and the calculated "-" curves is sufficiently good to lend credence to the model adopted. It can be improved (or made worse) by changing γ, T, or l. This, we feel, is not worth doing, because the

actual experimental geometry is cylindrical and not planar, and not enough is known about actual density distribution in the presence of a magnetic field.

We wish to thank Dr. J. A. Morrison and Dr. J. McKenna for helpful discussions regarding the validity of the method used in solving the Boltzmann equation.

[1]K. Mitani, H. Kubo, and S. Tanaka, J. Phys. Soc. Japan 19, 211 (1964).

[2]I. B. Bernstein, Phys. Rev. 109, 10 (1958).

[3]J. Nickel, J. Parker, and R. W. Gould, Phys. Rev. Letters 11, 183 (1963).

[4]A. Dattner, Ericsson Technics 8, 1 (1963); F. W. Crawford, Phys. Letters 5, 244 (1963); A. M. Messiaen and P. E. Vandeplass, Physica 28, 537 (1963); F. C. Hoh, Phys. Rev. 133, A1016 (1964).

[5]S. J. Buchsbaum, L. Mower, and S. C. Brown, Phys. Fluids 3, 806 (1960).

[6]G. E. Bekefi, J. D. Coccoli, E. B. Hooper, and S. J. Buchsbaum, Phys. Rev. Letters 9, 6 (1962).

[7]A. Simon and M. N. Rosenbluth, Phys. Fluids 6, 1566 (1963); S. J. Buchsbaum, Bull. Am. Phys. Soc. 9, 317 (1964).

[8]In the linearized Boltzmann equation we neglected the linear term f_1E_0 as compared with the term f_0E_1, where the subscripts 0 and 1 refer to unperturbed and perturbed quantities. Dimensional analysis shows that the neglected term is of the order $(l_D/\lambda)^2$ smaller than f_0E_1, where l_D is the Debye length and λ is a measure of the wavelength of the oscillation.

[9]This method may be used to solve the Boltzmann-Maxwell equation for arbitrary finite geometries. The details of the method will be published elsewhere.

[10]For resonances near $\omega = n\omega_c$ with $n \geq 3$, successively higher powers of T need to be retained.

[11]H. Bateman, Higher Transcendental Functions (McGraw-Hill Book Company, Inc., New York, 1953), Vol. 2.

SUPERCONDUCTIVITY OF TUNGSTEN

J. W. Gibson and R. A. Hein
U. S. Naval Research Laboratory, Washington, D. C.
(Received 1 May 1964)

Superconductivity has been observed in a sample of high-purity tungsten. At present our data indicate that the superconducting-to-normal transition occurs at a temperature less than 0.011°K. (Calculations suggest a lower limit of 0.005°K.) The data were obtained with the sample in zero external magnetic field using a dc measuring field of 0.10 oersted. A measuring field of 0.2 oersted is sufficient to drive the tungsten normal at the lowest temperature reached. The extremely low temperature necessary to observe the transition was produced by adiabatic demagnetization of about 28 grams of potassium chrome alum which had been allowed to crystallize around a system of copper wires. The single-crystal, high-purity tungsten sample was tightly enmeshed in these wires about 8 cm below the salt by using G.E. 7031 adhesive and nylon thread. Susceptibility of the salt and the tungsten were independently observed by a dc mutual inductance coil system and a ballistic type galvanometer.[1] Figure 1(a) shows the tungsten transition as the system warms up from the lowest temperature achieved. Galvanometer deflections (which are a linear function of the susceptibility) are plotted versus elapsed time after demagnetization. Figure 1(b) shows the changes in susceptibility of the potassium chrome alum for the same time intervals. Notice that the superconducting-to-normal transition of the tungsten occurs before the salt reaches its maximum susceptibility, which has been determined to be 0.011°K.[2]

A superconducting-to-normal transition was observed in two separate experiments. After the initial observation of the superconductivity of tungsten (Run 1), we failed in our efforts to reproduce these data, i.e., to observe superconductivity at all in the tungsten, until our ninth run five months later. We now believe that the main problem was one of reproducing the good thermal contact between the grown chrome alum and the copper wires that was achieved in the earlier experiment. Hence, we were not cooling the tungsten to a low enough temperature. By systematic investigation we now believe that we have devised a much more satisfactory technique for achieving good thermal contact, and this was manifest by the success of our Run 9 experiment with tungsten. A comparison of the two transitions is shown in Fig. 2. Both transitions occur at a temperature less than that of the maximum susceptibility of the salt (0.011°K). We believe these data